

Contribution from the Department of Chemistry,
University of Alberta, Edmonton, Alberta, Canada T6G 2G2

Stereochemically Nonrigid Six-Coordinate Metal Carbonyl Complexes. 3. The Series *cis*-Fe(CO)₄(SnR₃)₂ (R = Me, Et, *n*-Pr, *n*-Bu, Ph, Cl) and the X-Ray Structure of Tetracarbonylbis(triphenylstannyl)iron(II)¹

R. K. POMEROY, L. VANCEA, H. P. CALHOUN, and W. A. G. GRAHAM*

Received November 3, 1976

AIC60789W

An investigation of the series *cis*-Fe(CO)₄(SnR₃)₂ (R = Me, Et, *n*-Pr, *n*-Bu, Ph, Cl), some of which had not been fully characterized previously, is described. ¹³C NMR spectroscopy shows that all but the chloro derivative are stereochemically nonrigid and that the barrier (ΔG^\ddagger) to axial-equatorial carbonyl averaging is approximately the same (10.8 kcal mol⁻¹) for all the organotin derivatives. From the three ¹³CO-Sn coupling constants observed in the low-temperature limiting spectrum, the ¹³CO resonance at lower field is assigned to the equatorial carbonyls for R = alkyl; the reverse is true for R = Ph, Cl. The carbonyl averaging process occurs without ligand dissociation as shown by the single averaged ¹³CO-Sn coupling in the high-temperature limiting spectrum. The latter coupling is a weighted average of the low-temperature values if one is assumed opposite in sign to the other two. The crystal and molecular structures of *cis*-Fe(CO)₄(SnPh₃)₂ have been determined. The compound crystallizes in the triclinic system with space group P $\bar{1}$; $a = 13.147$ (6), $b = 10.988$ (4), $c = 12.875$ (6) Å; $\alpha = 83.43$ (4), $\beta = 80.92$ (3), $\gamma = 82.30$ (4)°; $Z = 2$. Full-matrix least-squares refinement gave a final R factor of 0.045 for the 3718 reflections measured by counter methods. The molecule exhibits marked deviation from octahedral geometry with Sn-Fe-Sn = 95.94 (4)° and CO_{axial}-Fe-CO_{axial} = 159.6 (4)°. The average Fe-Sn bond length is 2.661 (1) Å.

Introduction

The barriers to polytopal rearrangement² of six-coordinate complexes are expected to be large, since an octahedral arrangement is normally thought to represent a considerable minimum on the potential energy surface.³ However, in the past few years such rearrangements have been shown to occur on the NMR time scale for three classes of six-coordinate compounds: (1) hydrides of the type ML₄H₂, where M = Fe or Ru and L is a trivalent phosphorus ligand;⁴ (2) certain tris chelates, including the tris(tropolonates) of aluminum and cobalt and tris(dithiocarbamates) of iron and ruthenium;⁵ (3) metal carbonyls of the type M(CO)₄(EMe₃)₂ where M = Fe, Ru, Os, and E = Si, Ge, Sn, Pb.^{1,6,7} It is striking that x-ray crystallography has shown, for at least one member of each class,⁸ a marked distortion from octahedral geometry in the solid state.

In the preceding papers of the present series,^{1,7} ¹³C NMR established the rapid permutation of axial and equatorial carbonyl groups¹² in *cis*-M(CO)₄(EMe₃)₂ molecules. In addition, coupling of ¹³C to the spin 1/2 isotopes of Si and Sn was preserved in the high-temperature limiting spectra of the iron derivatives, directly verifying the polytopal character of the process. In the low-temperature limiting spectra, spin-spin coupling in the tin and lead derivatives led to the assignment of the ¹³CO resonance at higher field as the equatorial carbonyl. However, this assignment of carbonyl resonances did not hold for *cis*-Fe(CO)₄(SnMe₃)₂.¹

In order to clear up this seeming anomaly, as well as to add to the body of knowledge concerning stereochemically nonrigid six-coordinate molecules, a systematic study of the series *cis*-Fe(CO)₄(SnR₃)₂ (R = Me, Et, *n*-Pr, *n*-Bu, Ph, Cl) has been carried out. In view of the possible relation between a distorted structure and a low permutational barrier, the crystal structure of one of these iron-tin compounds, *cis*-Fe(CO)₄(SnPh₃)₂, has been determined.

Experimental Section

All experiments were carried out under an atmosphere of dry, oxygen-free argon or nitrogen. Hydrocarbon solvents were distilled from calcium hydride or potassium benzophenone ketyl and saturated with nitrogen or argon before use. NMR solvents were dried over type 4A molecular sieves. The dioxane solvate of disodium tetracarbonylferrate(-II), Na₂Fe(CO)₄·1.5C₄H₈O₂, was purchased as "Collman's Reagent" from Ventron Corp. (Alfa Products). The

Table I. Elemental Analysis and Molecular Weights^a

Compd	Calcd			Found		
	Mol wt	% C	% H	Mol wt	% C	% H
Fe(CO) ₄ (SnMe ₃) ₂	496	24.24	3.66	496		
Fe(CO) ₄ (SnEt ₃) ₂	580	33.15	5.22	580	33.65	5.19
Fe(CO) ₄ (SnPr ₃) ₂	664	39.81	6.38	664	40.45	6.22
Fe(CO) ₄ (SnBu ₃) ₂	748	44.96	7.28	748	46.45	7.89

^a Determined by mass spectrometer. Values quoted refer to the most intense peak of the isotopic multiplet due to the particular ion.

organotin starting materials were commercially available and were used without further purification.

Infrared spectra were recorded using a Perkin-Elmer Model 337 grating spectrometer with scale expansion calibrated with carbon monoxide gas. Mass spectra were obtained using an Associated Electrical Industries MS-9 or modified MS-2 instrument. Direct introduction of samples was employed. Computer-simulated isotope combination patterns¹³ were in excellent agreement with those observed for the parent ions of the new compounds. Carbon-13 NMR spectra were recorded using a Bruker HFX-90-Nicolet 1085 spectrometer; operating details have been described.¹ A relaxation reagent, tris(acetylacetonato)chromium(III), was used only in the case of *cis*-Fe(CO)₄(SnCl₃)₂. Approximate ΔG^\ddagger values were calculated using the relationships $\tau = 1/\pi(2)^{1/2}\Delta\nu$ and $1/2\tau = \kappa(kT/h) \exp(-\Delta G^\ddagger/RT)$, where T is the coalescence temperature and $\Delta\nu$ the chemical shift difference in the low temperature limiting spectrum. The other symbols have their customary significance. In earlier papers of this series,^{1,7} the rate of exchange was taken as $1/\tau$ rather than $1/2\tau$, resulting in a systematic error of approximately 3% in ΔG^\ddagger . Values of ΔG^\ddagger around 10–12 kcal mol⁻¹ should be 0.3 kcal mol⁻¹ higher, and those near 17 kcal mol⁻¹ should be 0.5 kcal mol⁻¹ higher in parts 1⁷ and 2.¹ We thank Dr. G. W. Grynkewich for bringing this error to our attention. Except for the case of the trimethyltin derivative (τ 9.50, CDCl₃), ¹H NMR spectroscopy was of little value in characterization since the compounds exhibited a complex multiplet near τ 9.

Microanalyses were performed by the microanalytical laboratory of this department. Results are presented in Table I. Some difficulty was encountered in obtaining satisfactory analyses since the alkyl derivatives are air-sensitive liquids which undergo slow redistribution reactions at room temperature.

Preparation of *cis*-Fe(CO)₄(SnBu₃)₂. To a sample of Na₂Fe(CO)₄·1.5C₄H₈O₂ (3.49 g, 10.1 mmol) in dry THF (25 mL) at -78 °C was added (*n*-Bu)₃SnCl (6.46 g, 19.8 mmol). The color changed at once from fawn to green, and stirring was continued for 20 min.

Table II. Infrared Data for *cis*-Fe(CO)₄(SnR₃)₂ Derivatives

Compd	Carbonyl str bands, ^a cm ⁻¹
Fe(CO) ₄ (SnMe ₃) ₂ ^b	2059 (8.4), 2001 (8.0), 1989 (3.8), 1972 (10)
Fe(CO) ₄ (SnEt ₃) ₂	2053 (8.4), 1996 (8.7), 1984 (4.7), 1964 (10)
Fe(CO) ₄ (SnPr ₃) ₂	2051 (9.2), 1993 (9.2), 1980 (5.0), 1962 (10)
Fe(CO) ₄ (SnBu ₃) ₂	2051 (8.7), 1993 (8.8), 1979 (4.3), 1962 (10)
Fe(CO) ₄ (SnPh ₃) ₂	2067 (9.8), 2011.5 (7.1), 2005 (6.4), 1984.5 (10)

^a In *n*-heptane solution. Relative intensities on a percent transmission scale are in parentheses. ^b Lit.¹⁴ values 2058, 1999, 1988, and 1970 cm⁻¹.

Solvent was then removed at room temperature, and *n*-hexane (40 mL) was added to the residue. The resulting mixture was filtered successively through a coarse and a fine glass frit. Hexane and any Fe(CO)₅ formed were then removed from the filtrate on a vacuum line, leaving *cis*-Fe(CO)₄(SnBu₃)₂ (7.5 g, 10.0 mmol). As obtained, the compound was a pale green or yellow air-sensitive liquid which appeared pure by infrared and ¹³C NMR spectroscopy. It was not sufficiently volatile to distill over a short path at 75 °C and 10⁻³ mm.

Preparation of Other Compounds. Reaction conditions were similar to those described above, with variations noted. Methyltin and ethyltin derivatives were purified by vacuum sublimation of crude material onto a probe cooled by liquid nitrogen; the compounds were obtained as pale yellow liquids on warming the probe. The methyl derivative has previously been reported,^{14,15} and the infrared spectra measured in this work (Table II) are in excellent agreement with the literature values. The ethyl derivative was prepared using Et₃SnBr; chlorotin derivatives were used in other cases. Yields in all cases were over 80%. The *n*-propyltin derivative underwent short-path-distillation only with difficulty at 75 °C (10⁻³ mm), and the ¹³C NMR spectrum was obtained on the crude material.

In the preparation of *cis*-Fe(CO)₄(SnPh₃)₂, CH₂Cl₂ was used instead of *n*-hexane for the extraction. This compound has previously been prepared¹⁶ although no infrared spectrum was reported.

The chloro derivative, *cis*-Fe(CO)₄(SnCl₃)₂, was prepared in this laboratory by the reaction of SnCl₄ with Fe(CO)₅ in benzene.¹⁷ In a slight modification of the earlier procedure, the reaction mixture was heated in a 200-mL Parr autoclave at 60 °C for 13 h.

Conversion of *cis*-Fe(CO)₄(SnR₃)₂ to [Fe(CO)₄SnR₂]₂. A sample of *cis*-Fe(CO)₄(SnMe₃)₂ after 1 week at -15 °C contained a small number of crystals; the infrared spectrum of the crystals (ν (CO) 2046, 1999, 1989 cm⁻¹) was identical with that of [Fe(CO)₄SnMe₂]₂.^{14,15} After 1 week at room temperature, *cis*-Fe(CO)₄(SnMe₃)₂ in a sealed vial had become a solid mass of yellow crystals. The mass spectra of some *cis*-Fe(CO)₄(SnR₃)₂ derivatives showed weak peaks due to [Fe(CO)₄SnR₂]₂, probably arising from this reaction at the inlet temperature (up to 100 °C) required to obtain a spectrum.

Enrichment with ¹³CO. Despite the good solubility of the organotin derivatives in the NMR solvents employed, even at low temperatures, enrichment with ¹³CO was usually necessary to observe clearly the ¹³C-^{117,119}Sn satellites. The following compounds were enriched by the method previously described:¹ Fe(CO)₄(SnMe₃)₂, Fe(CO)₄(SnBu₃)₂, and Fe(CO)₄(SnPh₃)₂. This method was not applicable to *cis*-Fe(CO)₄(SnCl₃)₂, which decomposed during ultraviolet irradiation; a suitably enriched sample was obtained by reaction of SnCl₄ with enriched Fe(CO)₅, prepared by the method of Noack and Ruch.¹⁸

Determination of the Crystal and Molecular Structure of *cis*-Fe(CO)₄(SnPh₃)₂. Crystals suitable for diffraction studies were obtained by slow crystallization from *n*-heptane. In addition to being air-sensitive, the crystals were slightly light sensitive; exposure to light was kept to a minimum during data collection.

Crystals were mounted in sealed capillaries in wax. Preliminary photographs indicated triclinic symmetry with space group *P* $\bar{1}$. A crystal of dimensions 0.24 × 0.10 × 0.48 mm was mounted in random orientation on a Picker four-circle FACS diffractometer. Cell dimensions ($a = 13.147$ (6), $b = 10.988$ (4), $c = 12.875$ (6) Å; $\alpha = 83.43$ (4), $\beta = 80.92$ (3), $\gamma = 82.30$ (4)°) were obtained by a least-squares fit of 12 high-angle reflections measured using Mo K α_1 (0.709 26 Å) radiation at 23 °C. The calculated density based on two molecules per unit cell is 1.591 g cm⁻³, in agreement with the experimental density of 1.59 g cm⁻³ determined by flotation in aqueous, nitrogen-saturated NaI solution.

Intensity data were measured using Mo K α radiation (λ 0.710 69 Å) which was monochromated by an oriented graphite crystal. All

reflections with 4° < 2 θ < 45° were measured using the θ -2 θ scan method with a scan width of 2° plus allowance for $\alpha_1 - \alpha_2$ dispersion at 1° min⁻¹. Background counts were taken for 20 s at the limits of the scan. Three standard reflections were measured every 100 reflections, and all three were observed to decrease in intensity linearly with time. Approximately halfway through the data collection the intensities of the standard reflections for the first crystal had decreased by 10%, when a second crystal, of dimensions 0.30 × 0.14 × 0.48 mm, was inserted. The decomposition was accompanied by a color change from colorless to brown. The intensities of the standard reflections for the second crystal had decreased by 6% by the end of data collection. The data for each crystal were corrected for decomposition (on the basis of the decay of the standards with time), for Lorentz and polarization effects, and were reduced to structure factor amplitudes with standard deviations estimated by the procedure of Doedens and Ibers,¹⁹ using a p factor of 0.05. Of 4731 independent reflections measured, 3718 were considered to be significantly above background ($I > 3\sigma(I)$, where $\sigma(I)$ was estimated from counting statistics). The data for the two crystals were corrected for absorption (the transmission factors ranged from 0.80 to 0.93 for the first crystal and from 0.78 to 0.89 for the second crystal) and placed on the same relative scale using the values of $|F_o|_{cor}$ for the 700 reflection (averages of 23 measurements for the first crystal and 7 measurements for the second crystal taken at the beginning of the data collection).

Structure Solution and Refinement. The space group was assumed to be *P* $\bar{1}$, and this was confirmed by the successful refinement in this space group. The positions of the iron and two tin atoms were determined from a three-dimensional sharpened Patterson map. A structure factor calculation gave $R = 27\%$, and an electron density map gave the positions of 41 additional nonhydrogen atoms. The remaining nonhydrogen atoms were located from a second difference map, and full-matrix least-squares refinement with anisotropic thermal parameters for Fe, Sn(1), and Sn(2) and isotropic thermal parameters for the other nonhydrogen atoms reduced R to 0.060 for 2819 reflections with 4° < 2 θ < 40° and $I > 3\sigma(I)$. Further refinement with anisotropic thermal parameters for Fe, Sn(1), Sn(2), C(1)-C(4), and O(1)-O(4), correction for anomalous dispersion effects for Fe, Sn(1), and Sn(2), and hydrogen atoms being placed in calculated positions reduced R and R_w to their final values, 0.045 and 0.060, respectively, for 3718 reflections with 4° < 2 θ < 45° and $I > 3\sigma(I)$. Hydrogen atom positions were calculated assuming a carbon-hydrogen distance of 1.02 Å, and the hydrogen atoms were given isotropic thermal parameters equal to those of the carbon atoms to which they were attached. The hydrogen atoms were included in the structure factor calculations but were not refined. On the final cycle of refinement no parameter shift was greater than 0.4 times its standard error. The standard deviation of an observation of unit weight based on 244 variables and 3718 observations was 1.99 electrons. A final electron density map showed no unusual features with all peaks less than 0.9 e Å⁻³.

The function minimized in the least-squares refinement was $\sum w(|F_o| - |F_c|)^2$ with $w = 1/\sigma^2(|F_o|)$. R and R_w are defined as $\sum ||F_o| - |F_c|| / \sum |F_o|$ and $[\sum w(|F_o| - |F_c|)^2 / \sum wF_o^2]^{1/2}$, respectively.

Atomic scattering factors for all nonhydrogen atoms²⁰ and hydrogen²¹ and the corrections for anomalous scattering for iron and tin²² were taken from the literature. Major computer programs used were a local modification of SFLSS by C. T. Prewitt, FORDAF by A. Zalkin, DATAP by P. Coppens, and ORTEP by C. K. Johnson.

Description of the Structure of *cis*-Fe(CO)₄(SnPh₃)₂

An overall view of the molecule is shown in Figure 1. Final positional and thermal parameters are given in Tables III and IV. Selected bond lengths and angles are listed in Table V.

It is apparent that the molecule is markedly distorted from octahedral geometry. The axial carbonyls¹² make an angle of 159.6 (4)° at iron, while the Sn(1)-Fe-Sn(2) angle is 95.94 (4)°. The angle C(2)-Fe-C(4) between the equatorial carbonyls is 92.0 (4)°, closer to the regular octahedral value.

The iron atom and the ligand atoms Sn(1), Sn(2), C(2), O(2), C(4), and O(4) are noticeably displaced from the equatorial plane. Thus, atoms C(2) and O(2) are below (-0.13 and -0.25 Å, respectively) and atoms C(4) and O(4) are above (0.20 and 0.36 Å) the plane defined by atoms Fe, Sn(1), and Sn(2). (The equation of this plane is -0.5684X - 0.5617Y +

Table III. Atomic Coordinates^a and Isotropic Temperature Factors

	<i>x</i>	<i>y</i>	<i>z</i>	<i>B</i> , Å ²
Fe	0.114 82 (8)	0.427 6 (1)	0.272 89 (8)	2.89 ^b
Sn(1)	0.260 90 (4)	0.340 46 (5)	0.393 09 (4)	2.92 ^b
Sn(2)	0.157 37 (4)	0.249 87 (5)	0.143 77 (4)	2.76 ^b
O(1)	0.288 1 (6)	0.553 6 (7)	0.157 3 (6)	5.95 ^b
O(2)	-0.034 5 (7)	0.543 1 (8)	0.134 1 (7)	8.15 ^b
O(3)	-0.005 0 (5)	0.237 7 (6)	0.395 2 (5)	4.48 ^b
O(4)	0.035 7 (5)	0.614 6 (6)	0.420 5 (5)	5.62 ^b
C(1)	0.223 5 (7)	0.501 9 (8)	0.201 2 (7)	3.92 ^b
C(2)	0.023 1 (8)	0.494 7 (9)	0.187 7 (8)	4.85 ^b
C(3)	0.043 8 (6)	0.310 8 (8)	0.348 8 (6)	3.23 ^b
C(4)	0.070 7 (7)	0.540 1 (8)	0.364 2 (7)	3.70 ^b
C(5)	0.217 4 (6)	0.214 1 (7)	0.527 5 (6)	3.23
C(6)	0.400 9 (6)	0.246 2 (8)	0.311 5 (6)	3.54
C(7)	0.305 0 (6)	0.496 1 (8)	0.456 9 (6)	3.28
C(8)	0.190 8 (6)	0.068 5 (7)	0.221 2 (5)	2.66
C(9)	0.275 4 (7)	0.282 3 (8)	0.010 1 (6)	3.83
C(10)	0.018 9 (6)	0.230 7 (7)	0.081 3 (6)	3.19
C(51)	0.186 5 (7)	0.101 9 (9)	0.517 8 (7)	4.19
C(52)	0.167 4 (8)	0.016 8 (9)	0.605 3 (8)	5.00
C(53)	0.175 2 (8)	0.045 (1)	0.702 5 (8)	5.78
C(54)	0.208 6 (8)	0.153 (1)	0.715 2 (8)	5.65
C(55)	0.231 6 (7)	0.237 3 (9)	0.628 1 (7)	4.88
C(61)	0.446 7 (7)	0.286 7 (9)	0.210 4 (7)	4.65
C(62)	0.444 9 (7)	0.137 7 (9)	0.362 0 (7)	4.34
C(63)	0.535 7 (9)	0.217 (1)	0.163 7 (9)	6.21
C(64)	0.577 4 (8)	0.113 (1)	0.216 2 (8)	5.69
C(65)	0.534 9 (8)	0.075 (1)	0.314 1 (8)	5.43
C(71)	0.243 8 (7)	0.550 6 (9)	0.541 0 (7)	4.56
C(72)	0.396 9 (7)	0.541 9 (8)	0.413 9 (7)	4.06
C(73)	0.275 3 (9)	0.647 (1)	0.583 6 (8)	5.91
C(74)	0.365 3 (9)	0.691 (1)	0.540 3 (9)	6.15
C(75)	0.425 1 (8)	0.643 (1)	0.458 8 (8)	5.21
C(81)	0.107 5 (6)	0.006 8 (8)	0.267 6 (6)	3.37
C(82)	0.121 8 (7)	-0.109 0 (8)	0.321 3 (7)	4.14
C(83)	0.220 8 (7)	-0.166 1 (9)	0.328 4 (7)	4.70
C(84)	0.305 1 (7)	-0.105 6 (9)	0.282 3 (7)	4.68
C(85)	0.290 0 (6)	0.009 7 (8)	0.229 4 (6)	3.50
C(91)	0.348 8 (9)	0.187 (1)	-0.020 8 (9)	5.89
C(92)	0.428 (1)	0.204 (1)	-0.105 (1)	7.43
C(93)	0.428 (1)	0.316 (2)	-0.158 (1)	9.28
C(94)	0.354 (1)	0.414 (1)	-0.136 (1)	8.98
C(95)	0.275 7 (9)	0.395 (1)	-0.045 7 (9)	6.27
C(101)	-0.081 4 (7)	0.262 4 (9)	0.126 8 (7)	4.88
C(102)	-0.168 (1)	0.245 (1)	0.081 (1)	6.94
C(103)	-0.151 (1)	0.193 (1)	-0.013 (1)	7.33
C(104)	-0.056 (1)	0.154 (1)	-0.060 (1)	8.99
C(105)	0.031 4 (9)	0.178 (1)	-0.012 8 (9)	6.42

^a Estimated standard deviation in the least significant figure given in parentheses in this and subsequent tables. ^b Equivalent isotropic thermal parameters; for anisotropic parameters, see Table IV.

0.6012*Z* = -2.0398, where *X*, *Y*, and *Z* are the orthogonal coordinates (Å.) The nonbonded contacts from Sn(1) to C(1), C(3), and C(4) are 2.94, 3.06, and 3.14 Å, respectively. The similar distances from Sn(2) to C(1), C(2), and C(3) are 3.21, 3.07, and 2.92 Å.

Table IV. Anisotropic Temperature Factors (Å²)^a

	<i>U</i> ₁₁	<i>U</i> ₂₂	<i>U</i> ₃₃	<i>U</i> ₁₂	<i>U</i> ₁₃	<i>U</i> ₂₃
Fe	0.0398 (6)	0.0297 (6)	0.0414 (6)	-0.0054 (5)	-0.0072 (5)	-0.0049 (5)
Sn(1)	0.0394 (4)	0.0335 (4)	0.0399 (3)	-0.0086 (3)	-0.0070 (3)	-0.0042 (2)
Sn(2)	0.0382 (3)	0.0342 (4)	0.0324 (3)	-0.0071 (3)	-0.0034 (2)	-0.0030 (2)
O(1)	0.070 (5)	0.069 (5)	0.084 (5)	-0.032 (4)	-0.006 (4)	0.019 (4)
O(2)	0.110 (7)	0.072 (6)	0.137 (7)	0.008 (5)	0.073 (6)	0.008 (5)
O(3)	0.060 (4)	0.053 (4)	0.057 (4)	-0.021 (3)	0.005 (3)	-0.010 (3)
O(4)	0.085 (5)	0.047 (4)	0.079 (5)	-0.007 (4)	0.006 (4)	-0.020 (4)
C(1)	0.058 (6)	0.035 (5)	0.056 (5)	-0.006 (5)	-0.015 (5)	0.003 (4)
C(2)	0.068 (7)	0.045 (6)	0.079 (7)	-0.001 (5)	-0.032 (6)	-0.011 (5)
C(3)	0.043 (5)	0.040 (5)	0.043 (5)	-0.011 (4)	-0.006 (4)	-0.014 (4)
C(4)	0.048 (5)	0.039 (5)	0.054 (5)	-0.006 (4)	-0.005 (4)	-0.008 (4)

^a The form of the thermal ellipsoid is $\exp[-2\pi^2(a^{*2}U_{11}h^2 + b^{*2}U_{22}k^2 + c^{*2}U_{33}l^2 + 2a^{*}b^{*}U_{12}hk + 2a^{*}c^{*}U_{13}hl + 2b^{*}c^{*}U_{23}kl)]$.

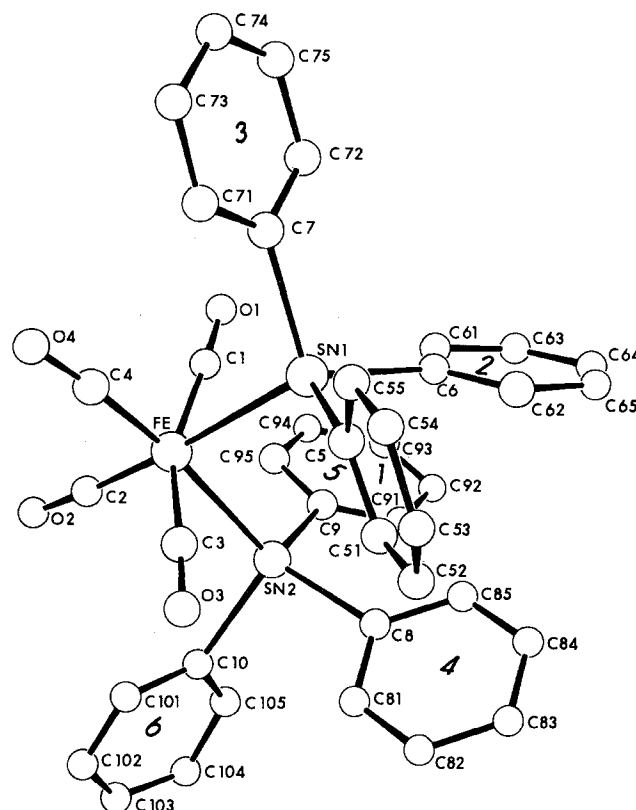


Figure 1. Molecular structure of *cis*-Fe(CO)₄(SnPh₃)₂. Numbers inside phenyl rings indicate designation in mean plane calculations (cf. supplementary data).

The structure invites comparison with that of *cis*-Fe(CO)₄(SiMe₃)₂.⁷ Distortion of the latter from octahedral is considerably more marked, with a CO_{ax}-Fe-CO_{ax} angle of 141.2 (1)° and a Si-Fe-Si angle of 111.8 (1)°. Also, the equatorial ligand atoms were coplanar and the nonbonded distances from silicon to the adjacent carbonyl carbons were approximately equal. It was useful to describe the geometry of the silyl derivative as a bicapped tetrahedron, with SiMe₃ groups as capping ligands. Both steric and electronic factors may be invoked to rationalize the distortion from regular octahedral. In particular, theoretical considerations have shown that in molecules of the type ML₄D₂, bicapped tetrahedral geometry is favored when D is a good σ donor and M is a d⁶ metal center.²³

It seems reasonable that a SiMe₃ ligand is a better σ donor than SnPh₃,²⁴ so that the tin derivative on electronic grounds should be less distorted. Examination of both structures also provides a rationale in terms of steric factors for the lesser distortion of the triphenyltin derivative. The Fe-Sn length is 0.2 Å longer than Fe-Si, and the phenyl groups can be

Table V. Selected Distances (Å) and Angles (deg) in $cis\text{-Fe}(\text{CO})_4(\text{SnPh}_3)_2$

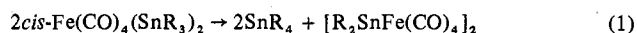
Bond Distances			
Fe-Sn(1)	2.666 (1)	C(4)-O(4)	1.157 (11)
Fe-Sn(2)	2.655 (1)	Sn(1)-C(5)	2.145 (8)
Fe-C(1)	1.813 (9)	Sn(1)-C(6)	2.167 (8)
Fe-C(2)	1.787 (10)	Sn(1)-C(7)	2.161 (8)
Fe-C(3)	1.795 (8)	Sn(2)-C(8)	2.145 (7)
Fe-C(4)	1.780 (9)	Sn(2)-C(9)	2.160 (8)
C(1)-O(1)	1.126 (12)	Sn(2)-C(10)	2.148 (8)
C(2)-O(2)	1.141 (13)	Mean C-C	1.38 (3)
C(3)-O(3)	1.150 (10)		
Angles			
Sn(1)-Fe-Sn(2)	95.94 (4)	C(5)-Sn(1)-C(7)	105.4 (3)
Sn(1)-Fe-C(1)	79.5 (3)	C(6)-Sn(1)-C(7)	107.2 (3)
Sn(1)-Fe-C(2)	175.6 (3)	Fe-Sn(2)-C(8)	114.3 (2)
Sn(1)-Fe-C(3)	84.3 (3)	Fe-Sn(2)-C(9)	114.9 (2)
Sn(1)-Fe-C(4)	87.3 (3)	Fe-Sn(2)-C(10)	108.6 (2)
Sn(2)-Fe-C(1)	89.8 (3)	C(8)-Sn(2)-C(9)	109.9 (3)
Sn(2)-Fe-C(2)	85.2 (3)	C(8)-Sn(2)-C(10)	101.2 (3)
Sn(2)-Fe-C(3)	79.6 (3)	C(9)-Sn(2)-C(10)	106.8 (3)
Sn(2)-Fe-C(4)	172.8 (3)	Sn(1)-C(5)-C(51)	122.3 (6)
C(1)-Fe-C(2)	96.2 (4)	Sn(1)-C(5)-C(55)	120.2 (6)
C(1)-Fe-C(3)	159.6 (4)	Sn(1)-C(6)-C(61)	123.4 (6)
C(1)-Fe-C(4)	97.2 (4)	Sn(1)-C(6)-C(62)	117.7 (6)
C(2)-Fe-C(3)	100.1 (4)	Sn(1)-C(7)-C(71)	121.6 (6)
C(2)-Fe-C(4)	92.0 (4)	Sn(1)-C(7)-C(72)	119.5 (6)
C(3)-Fe-C(4)	94.4 (4)	Sn(2)-C(8)-C(81)	117.5 (5)
Fe-C(1)-O(1)	176.6 (8)	Sn(2)-C(8)-C(85)	124.6 (5)
Fe-C(2)-O(2)	176.8 (9)	Sn(2)-C(9)-C(91)	119.6 (7)
Fe-C(3)-O(3)	177.1 (7)	Sn(2)-C(9)-C(95)	120.5 (7)
Fe-C(4)-O(4)	175.2 (8)	Sn(2)-C(10)-C(101)	126.7 (6)
Fe-Sn(1)-C(5)	116.8 (2)	Sn(2)-C(10)-C(105)	116.9 (7)
Fe-Sn(1)-C(6)	115.2 (2)	Mean C-C-C	120.0 (18)
Fe-Sn(1)-C(7)	107.4 (2)		
C(5)-Sn(1)-C(6)	104.2 (3)		

oriented so that their smaller dimension is most advantageously used;²⁷ both factors permit a smaller Sn-Fe-Sn angle than Si-Fe-Si. In addition, the ortho hydrogen atoms occupy positions above and below the Sn-Fe-Sn triangle which are empty in $cis\text{-Fe}(\text{CO})_4(\text{SiMe}_3)_2$; in consequence, while the axial carbonyls in the silicon compound moved into an open "pocket" above and below the $\text{Fe}(\text{SiMe}_3)_2$ fragment, such a pocket is lacking in the tin structure. The iron-tin bond lengths of 2.666 (1) and 2.655 (1) Å are typical of values previously observed,²⁸ while the average tin-carbon distance of 2.154 (9) Å is equal to that found in $\text{Ph}_3\text{SnMn}(\text{CO})_5$.²⁹ There are no abnormally short intermolecular contacts.

Results and Discussion

The compounds $cis\text{-Fe}(\text{CO})_4(\text{SnR}_3)_2$, where R = Me, Et, *n*-Pr, *n*-Bu, or Ph, were obtained in yields of 80% or higher from the reaction of the chloro- or bromostannanes with $\text{Na}_2\text{Fe}(\text{CO})_4 \cdot 1.5\text{C}_4\text{H}_8\text{O}_2$ in tetrahydrofuran at -78 °C. The compounds undergo slow decomposition, in some cases at or

below room temperature, according to eq 1. This reaction



was observed for R = Me at 140 °C¹⁴ and in the alkyllead series was so favored that mononuclear alkyl compounds $\text{Fe}(\text{CO})_4(\text{PbR}_3)_2$ could not be isolated.³⁰ Our attempts to prepare $\text{Fe}(\text{CO})_4(\text{PbPh}_3)_2$, a known compound,³⁰ by the method used for the tin derivative led only to binuclear $[\text{Ph}_2\text{PbFe}(\text{CO})_4]_2$, confirming the greater ease of decomposition in the lead series.

Infrared spectra of the iron-tin derivatives (Table II) show four carbonyl stretching bands, consistent with a *cis* geometry. There was no evidence from infrared or NMR spectra for the presence of a *trans* isomer.

An interesting feature of the infrared spectra is the relatively high intensity of the carbonyl stretching fundamental at highest frequency. This band would normally be assigned (under idealized C_{2v} symmetry) as the A_1 mode involving mainly the symmetric motion of the axial carbonyl groups and would be expected on the basis of a sum of local dipoles argument to be weak.³¹ We suggest that it gains intensity in $cis\text{-Fe}(\text{CO})_4(\text{SnR}_3)_2$ molecules due to nonlinearity of the axial carbonyl groups, as observed in the $cis\text{-Fe}(\text{CO})_4(\text{SnPh}_3)_2$ structure.

¹³C NMR Spectra. Chemical shift data for the tin-iron derivatives are presented in Table VI. The carbonyl chemical shifts are in the range 206–209 ppm for the organotin derivatives but are more shielded in $cis\text{-Fe}(\text{CO})_4(\text{SnCl}_3)_2$. The carbon atoms of the organic substituents show a larger variation; these resonances were assigned by using the off-resonance decoupling technique and by comparison of carbon-tin coupling constants with those of the parent organotin halides.

Chemical shifts and coupling constants of the organotin halides are given in Table VII. A comparison of the alkyl derivatives shows that in the iron derivatives, C(1) is shifted about 3 ppm upfield, C(2) is shifted about 2 ppm downfield, and C(3) and C(4) are shifted about 1 ppm downfield relative to the parent trialkyltin chlorides.

The ¹³C resonances due to the carbon atoms of the organic groups in $cis\text{-Fe}(\text{CO})_4(\text{SnR}_3)_2$ (R = Et, *n*-Pr, *n*-Bu) are well-resolved sharp lines at room temperature. At low temperature, some broadening occurs. For example, the half-widths of the C(1)-C(4) peaks of $cis\text{-Fe}(\text{CO})_4(\text{SnBu}_3)_2$ are 5.5, 4.3, 3.6, and 3.5 Hz, respectively, at -80 °C. A viscosity effect may be ruled out since the TMS reference is still sharp (1.6 Hz). It seems reasonable to attribute this to restricted rotation. In all cases it was the resonance of the carbon atom furthest from the tin which showed the least broadening.

A similar effect was noted in the phenyl carbon resonances of $cis\text{-Fe}(\text{CO})_4(\text{SnPh}_3)_2$ at -90 °C. In this case the resonance

Table VI. ¹³C Chemical Shifts in $cis\text{-Fe}(\text{CO})_4(\text{SnR}_3)_2$ Derivatives^a

Compd	CO _{ax}	CO _{eq}	C(1)	C(2)	C(3)	C(4)	Temp, K
$\text{Fe}(\text{CO})_4(\text{SnMe}_3)_2$	207.86	208.07	-3.67				163 ^b
		207.75	-3.29				273 ^c
		207.75	-3.24				293 ^b
		208.07	-2.75				300
$\text{Fe}(\text{CO})_4(\text{SnEt}_3)_2$	207.42	208.40	6.31	11.81			193
		207.91	7.44	11.60			303
$\text{Fe}(\text{CO})_4(\text{SnPr}_3)_2$	207.69	208.50	17.26	21.36	19.58		193
		208.13	18.77	21.36	19.15		303
$\text{Fe}(\text{CO})_4(\text{SnBu}_3)_2$	207.75	208.69	14.54	29.86	28.16	14.21	193
		208.13	15.75	29.99	27.78	13.70	303
$\text{Fe}(\text{CO})_4(\text{SnPh}_3)_2$	206.72	206.45	140.69	137.08	128.93	129.35	183
		206.78	141.56	137.08	128.82	129.15	303
$\text{Fe}(\text{CO})_4(\text{SnCl}_3)_2$	195.29	195.18					293

^a Chemical shifts in ppm downfield from TMS. Solvent is CD_2Cl_2 except as noted. The carbon attached to tin is taken as C(1).

^b CD_2Cl_2 -methylcyclohexane-*d*₁₄ (1:1) as solvent. ^c Toluene-*d*₈ solvent.

Table VII. ^{13}C Chemical Shifts^a and Coupling Constants^b in R_3SnX Derivatives

Compd	Chem shift				^{13}C - $^{117,119}\text{Sn}$ coupling const			
	C(1)	C(2)	C(3)	C(4)	C(1)	C(2)	C(3)	C(4)
Me_3SnCl	-0.70				364, 381			
Me_3SnCl^c	0.0				386			
Me_3SnCl^d	-0.7				365, 379			
Et_3SnCl^c	9.3	9.9			352	26		
Pr_3SnCl	20.66	19.58	18.45		326, 341	23	63	
Bu_3SnCl	17.75	28.16	27.08	13.70	325, 341	24	65	
Ph_3SnCl	137.67	136.38	129.44	130.79	592, 618	49	63	13
Ph_3SnCl^c	137.5	136.1	129.2	130.5	610	49	68	12

^a Chemical shifts in ppm downfield from TMS. Solvent is CD_2Cl_2 . Temperature is 303 K. The carbon attached to tin is taken as C(1).
^b Values in hertz. Values separated by commas indicate ^{117}Sn and ^{119}Sn couplings. Otherwise, the average value is given. ^c Values from T. N. Mitchell, *J. Organomet. Chem.*, 59, 189 (1973). Solvent is CDCl_3 . ^d Values from G. Singh, *J. Organomet. Chem.*, 99, 251 (1975). Solvent is CDCl_3 .

Table VIII. ^{13}C - $^{117,119}\text{Sn}$ Coupling Constants in *cis*- $\text{Fe}(\text{CO})_4(\text{SnR}_3)_2$ Derivatives^a

Compd	Carbonyl groups				Organic group			
	$\text{CO}_{\text{ax-Sn}}$	$\text{CO}_{\text{eq-Sncis}}$	$\text{CO}_{\text{eq-Sntrans}}$	Av obsd (calcd) ^b	C(1)	C(2)	C(3)	Temp, K
$\text{Fe}(\text{CO})_4(\text{SnMe}_3)_2$	101	65	-33	60 (58.5)	262, 274			163 ^c 293 ^c
$\text{Fe}(\text{CO})_4(\text{SnEt}_3)_2$	98	62	-26	59 (58.0)	260, 272	23		193 303
$\text{Fe}(\text{CO})_4(\text{SnPr}_3)_2$	97	65	-26	59 (58.3)	259, 271	24		193 303
$\text{Fe}(\text{CO})_4(\text{SnBu}_3)_2$	96	61	-25	59 (57.0)	252, 263	21	67	193 303
$\text{Fe}(\text{CO})_4(\text{SnPh}_3)_2$	107, 112	80	-43	66 (64.1)	251, 263	21	66	183 303
$\text{Fe}(\text{CO})_4(\text{SnCl}_3)_2$	224, 235	170	-37		398, 416	36	47	183 303
					397, 416	38	50	303

^a Values in hertz. Values separated by commas indicate ^{117}Sn and ^{119}Sn couplings. Otherwise, the average value is given. Solvent is CD_2Cl_2 except as noted. Signs of coupling constants are relative only (see text). The carbon attached to tin is taken as C(1). ^b $J_{\text{av}}(\text{calcd}) = 0.25 [2J(\text{CO}_{\text{ax-Sn}}) + J(\text{CO}_{\text{eq-Sncis}}) + J(\text{CO}_{\text{eq-Sntrans}})]$. ^c CD_2Cl_2 -methylcyclohexane- d_{14} (1:1) solvent.

due to C(1) remained sharp at 2.5 Hz while C(2) and C(3) resonances broadened to 8.8 and 9.5 Hz, respectively. The C(4) peak was obscured by the C(3) absorption. Again, restricted rotation is a possible explanation, either about the tin-carbon bond or the tin-iron bond.

In most cases, the infrared carbonyl stretching bands were broader than usually found in metal carbonyl complexes. This is also consistent with a range of conformations for the molecules.

Axial and Equatorial Carbonyl Assignments. As pointed out previously,¹ two pairs of ^{13}C - $^{117,119}\text{Sn}$ spin-spin coupling satellites are expected for the equatorial carbonyl resonance, but only one pair (at twice the intensity) is expected for the axial carbonyl signal. The earlier work with compounds such as *cis*- $\text{Ru}(\text{CO})_4(\text{EMe}_3)_2$ and *cis*- $\text{Os}(\text{CO})_4(\text{EMe}_3)_2$ (E = Sn, Pb) showed that the resonance of the equatorial carbonyls (those trans to the one-electron donors) is at higher field. At the time, *cis*- $\text{Fe}(\text{CO})_4(\text{SnMe}_3)_2$ was recognized as an exception,¹ and it was in part to clarify the validity of generalizations about carbonyl chemical shifts that the present work was undertaken.

Figure 2 shows the ^{13}C NMR spectrum (carbonyl region) of *cis*- $\text{Fe}(\text{CO})_4(\text{SnBu}_3)_2$, and Figure 3 that of *cis*- $\text{Fe}(\text{CO})_4(\text{SnPh}_3)_2$. Both compounds have been enriched with ^{13}C in order to determine the coupling constants more accurately. It is clear from Figure 2 that in the tri-*n*-butyltin derivative, the equatorial carbonyl signal lies at lower field; the other trialkyltin complexes (*cis*- $\text{Fe}(\text{CO})_4(\text{SnMe}_3)_2$, *cis*- $\text{Fe}(\text{CO})_4(\text{SnEt}_3)_2$, and *cis*- $\text{Fe}(\text{CO})_4(\text{SnPr}_3)_2$) follow the same "anomalous" pattern. On the other hand, the triphenyltin derivative, as Figure 3 shows, has the equatorial signal at higher field, as does *cis*- $\text{Fe}(\text{CO})_4(\text{SnCl}_3)_2$; this pattern is the one observed for the ruthenium and osmium compounds of tin and lead so far studied.¹

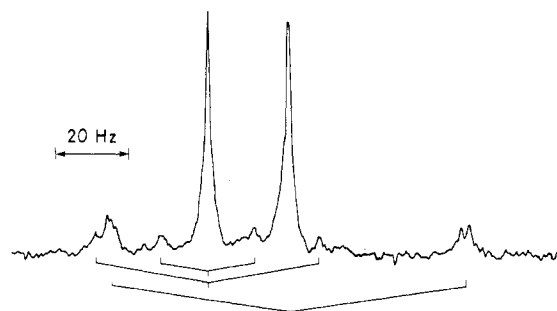


Figure 2. Carbonyl region of the ^{13}C NMR spectrum of ^{13}C -enriched *cis*- $\text{Fe}(\text{CO})_4(\text{SnBu}_3)_2$ (CD_2Cl_2 , -90°C). Satellites due to ^{13}C - $^{117,119}\text{Sn}$ coupling are marked and establish that resonance at lower field is due to equatorial carbonyls.

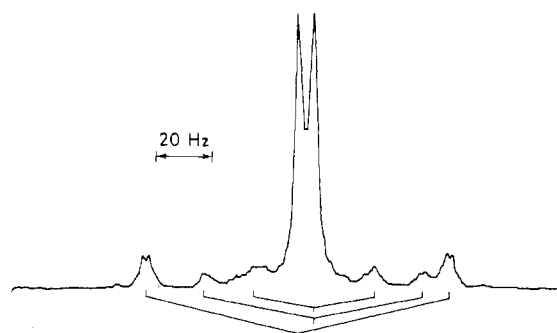


Figure 3. Carbonyl region of the ^{13}C NMR spectrum of *cis*- $\text{Fe}(\text{CO})_4(\text{SnPh}_3)_2$ (CD_2Cl_2 , -90°C). Satellites due to ^{13}C - $^{117,119}\text{Sn}$ coupling are marked and establish that resonance at higher field is due to equatorial carbonyls.

Table IX. Coalescence Temperatures and Free Energies of Activation for Axial-Equatorial Averaging in $cis\text{-Fe}(\text{CO})_4(\text{SnR}_3)_2$ Derivatives^a

Compd	$\Delta\delta$, Hz	Coalescence temp., °C	ΔG^\ddagger (at coalescence), kcal mol ⁻¹
$\text{Fe}(\text{CO})_4(\text{SnMe}_3)_2$	4.7	-75	10.5 ^b
$\text{Fe}(\text{CO})_4(\text{SnEt}_3)_2$	22.1	-50	11.2
$\text{Fe}(\text{CO})_4(\text{SnPr}_3)_2$	18.3	-60	10.8
$\text{Fe}(\text{CO})_4(\text{SnBu}_3)_2$	21.2	-50	11.2
$\text{Fe}(\text{CO})_4(\text{SnPh}_3)_2$	6.1	-73	10.5
$\text{Fe}(\text{CO})_4(\text{SnCl}_3)_2$	2.5	>20	>16.1

^a From ¹³C NMR spectra. $\Delta\delta$ is the chemical shift difference between axial and equatorial carbonyl groups in the low-temperature limiting spectrum. Solvent is CD_2Cl_2 except as noted.

^b CD_2Cl_2 -methylcyclohexane-*d*₁₄ (1:1) solvent.

Coupling Constants. Carbon-13 to ^{117,119}Sn coupling constants are given in Table VIII. ² $J(^{13}\text{CO}_{\text{ax}}\text{-Sn})$ may be uniquely assigned on an intensity basis and in all cases was greater in magnitude than the other two. Of the two possible coupling constants involving the equatorial carbonyls, designated ² $J(\text{CO}_{\text{eq}}\text{-Sn}_{\text{cis}})$ and ² $J(\text{CO}_{\text{eq}}\text{-Sn}_{\text{trans}})$, the one with the same sign (see below) as the axial carbon coupling is assigned as ² $J(\text{CO}_{\text{eq}}\text{-Sn}_{\text{cis}})$, since the geometric relationship of both interactions is similar (i.e., both are *cis*). The one of opposite sign may therefore be attributed to the trans coupling, ² $J(\text{CO}_{\text{eq}}\text{-Sn}_{\text{trans}})$.

A single averaged pair of spin-spin coupling satellites was observed in the high-temperature limiting spectra. Comparison with the weighted average of the three ² $J(^{13}\text{CO}\text{-Sn})$ couplings observed at low temperature led to the conclusion that the smallest coupling, assigned as ² $J(^{13}\text{CO}_{\text{eq}}\text{-Sn}_{\text{trans}})$, is of opposite sign to the other two. Averaged coupling constants calculated on this basis are compared with the observed value in Table VIII.

It is of interest that two of the coupling constants in $cis\text{-Fe}(\text{CO})_4(\text{SnCl}_3)_2$ are roughly twice the size of those in the organotin derivatives. Also, the ¹ $J(\text{C}\text{-Sn})$ coupling constants of the organic groups are significantly smaller than the corresponding values in the parent organotin chlorides. Both observations are consistent with the isovalent hybridization of tin so that the s character of the orbitals directed toward its more electropositive substituents is enhanced.³² Qualitatively, spin-spin coupling is expected to be greater the more s character is involved in the relevant bonding orbitals.

Stereochemical Nonrigidity of $\text{Fe}(\text{CO})_4(\text{SnR}_3)_2$ Derivatives. At temperatures below -50 °C, two ¹³CO resonances are observed for the $cis\text{-Fe}(\text{CO})_4(\text{SnR}_3)_2$ compounds (R = Me, Et, *n*-Pr, *n*-Bu, Ph). As the temperature is increased, these peaks broaden and finally coalesce to a single peak above 0 °C. This is essentially the behavior reported earlier¹ for $\text{Fe}(\text{CO})_4(\text{EMe}_3)_2$ (E = Si, Ge, or Sn); i.e., the molecules are stereochemically nonrigid. Similarly to $cis\text{-Fe}(\text{CO})_4(\text{SnMe}_3)_2$, the tin to carbonyl couplings are retained at high temperatures, and furthermore the compounds do not exchange with ¹³CO under the same conditions. These observations constitute strong evidence that the rearrangement is nondissociative.

The gross features of the permutation mechanism for compounds of this class have been identified in the preceding papers of this series.^{1,7} It involves a *cis* to *trans* to *cis* sequence, and it is not necessary that detectable amounts of the *trans* isomer be present. In the alkyltin-iron complexes described here, only the *cis* isomer is detectable.

Values of the free energy of activation are listed in Table IX.³³ Along the series R = Me, Et, *n*-Pr, *n*-Bu, and Ph, ΔG^\ddagger does not vary significantly. In contrast, the trichlorotin derivative is rigid at room temperature. An increase in carbonyl permutation barriers with halogen substitution is particularly

clear in the series $cis\text{-Fe}(\text{CO})_4(\text{SiCl}_n\text{Me}_{3-n})_2$ ($n = 0-3$).¹ An interesting, although scarcely surprising, fact is that substituent effects on carbonyl permutation in the five-coordinate compounds $\text{X}_3\text{SnCo}(\text{CO})_4$ are quite different; in the latter it appears that the barrier is lowest when X = Cl and higher for X = alkyl.³⁴

There is a correlation between ¹³CO chemical shifts and permutation barriers in the $cis\text{-M}(\text{CO})_4(\text{ER}_3)_2$ series: the larger the chemical shift value, the lower the barrier.³⁵ This trend is best shown by the series $cis\text{-Fe}(\text{CO})_4(\text{SiCl}_n\text{Me}_{3-n})_2$ ($n = 0-3$),¹ and the results of the present work are consistent; the average chemical shift of the trialkyltin derivatives is 11-13 ppm greater than that for $cis\text{-Fe}(\text{CO})_4(\text{SnCl}_3)_2$.

Conclusions

The structure of $cis\text{-Fe}(\text{CO})_4(\text{SnPh}_3)_2$ exhibits a distortion toward bicapped tetrahedral, although to a lesser extent than does $cis\text{-Fe}(\text{CO})_4(\text{SiMe}_3)_2$. Yet the average barrier for carbonyl permutation in these compounds and the four alkyltin derivatives examined is 10.9 kcal mol⁻¹, and all values are within 0.4 kcal mol⁻¹ of the mean. Thus the intuitively appealing possibility of a relation between barrier height and degree of distortion from octahedral geometry remains to be rigorously established. We continue to pursue this notion. One may note, as a further datum, that the barrier height for *cis*-*trans* isomerization in $\text{Ru}(\text{CO})_4(\text{GeCl}_3)_2$ is great enough that there is no isomerization in solution at room temperature over many days and that both the *cis* and *trans* isomers possess structures close to regular octahedral.³⁶

Finally, assignments of axial and equatorial ¹³CO resonances in iron complexes of the type $cis\text{-Fe}(\text{CO})_4(\text{SiR}_3)_2$ and $cis\text{-Fe}(\text{CO})_4(\text{GeR}_3)_2$ —where there is no independent evidence from spin satellites—must be regarded as uncertain. For ruthenium and osmium analogues, where the axial-equatorial chemical shift separation is larger (100-200 Hz compared with 2-40 Hz), reversals due to substituent variations are unlikely and it appears to be a useful guide that “the ¹³C resonance of the carbonyl *trans* to the one-electron donor ligand is at higher field”.¹

Acknowledgment. We thank the National Research Council of Canada for financial support and for a postdoctoral fellowship to H.P.C. We thank Dr. J. S. Martin for a helpful discussion and Dr. T. T. Nakashima for invaluable assistance and comments on the NMR aspects of the work.

Registry No. $cis\text{-Fe}(\text{CO})_4(\text{SnMe}_3)_2$, 18372-97-9; $cis\text{-Fe}(\text{CO})_4(\text{SnEt}_3)_2$, 61788-07-6; $cis\text{-Fe}(\text{CO})_4(\text{SnPr}_3)_2$, 61788-08-7; $cis\text{-Fe}(\text{CO})_4(\text{SnBu}_3)_2$, 61788-09-8; $cis\text{-Fe}(\text{CO})_4(\text{SnPh}_3)_2$, 21868-08-6; $cis\text{-Fe}(\text{CO})_4(\text{SnCl}_3)_2$, 19601-41-3; Me_3SnCl , 1066-45-1; Pr_3SnCl , 2279-76-7; Bu_3SnCl , 1461-22-9; Ph_3SnCl , 639-58-7; $\text{Na}_2\text{Fe}(\text{CO})_4$, 16182-63-1; $[\text{Fe}(\text{CO})_4\text{SnMe}_2]_2$, 15615-58-4; ¹³C, 14762-74-4.

Supplementary Material Available: Calculated hydrogen atom positions, selected intermolecular distances, mean planes through the phenyl rings, packing diagram, calculated and observed structure factor amplitudes (22 pages).

References and Notes

- (1) Part 2: L. Vancea, R. K. Pomeroy, and W. A. G. Graham, *J. Am. Chem. Soc.*, **98**, 1407 (1976).
- (2) E. L. Muettterties, *J. Am. Chem. Soc.*, **91**, 1636 (1969). This useful term implies that there is no change in coordination number during ligand permutation; lack of metal-ligand bond breaking is an essential feature.
- (3) E. L. Muettterties, *J. Am. Chem. Soc.*, **90**, 5097 (1968); J. P. Jesson and E. L. Muettterties, *Dyn. Nucl. Magn. Reson. Spectrosc.*, 277 (1975).
- (4) F. N. Tebbe, P. Meakin, J. P. Jesson, and E. L. Muettterties, *J. Am. Chem. Soc.*, **92**, 1068 (1970); P. Meakin, E. L. Muettterties, F. N. Tebbe, and J. P. Jesson, *ibid.*, **93**, 4701 (1971); P. Meakin, E. L. Muettterties, and J. P. Jesson, *ibid.*, **95**, 75 (1973).
- (5) R. H. Holm, *Dyn. Nucl. Magn. Reson. Spectrosc.*, Chapter 9 (1975). This excellent review includes a “proviso” with respect to chelate compounds on p 372 which should not be forgotten.
- (6) R. K. Pomeroy and W. A. G. Graham, *J. Am. Chem. Soc.*, **94**, 274 (1972).

- (7) L. Vancea, M. J. Bennett, C. E. Jones, R. A. Smith, and W. A. G. Graham, *Inorg. Chem.*, **16**, 897 (1977).
- (8) The reported structures are *cis*-Fe[PPh(OEt)₂]₄H₂,⁹ tris(tropolonato)aluminum(III),¹⁰ Fe(S₂CN(Et)₂)₂S₂C₂(CF₃)₂,¹¹ and *cis*-Fe(CO)₄(SiMe₃)₂.⁷
- (9) P. Meakin, L. J. Guggenberger, J. P. Jesson, D. H. Gerlach, F. N. Tebbe, W. G. Peet, and E. L. Muetterties, *J. Am. Chem. Soc.*, **92**, 3482 (1970); L. J. Guggenberger, D. D. Titus, M. T. Flood, R. E. Marsh, A. A. Orio, and H. B. Gray, *ibid.*, **94**, 1135 (1972).
- (10) E. L. Muetterties and L. J. Guggenberger, *J. Am. Chem. Soc.*, **94**, 8046 (1972).
- (11) D. L. Johnston, W. L. Rohrbaugh, and W. D. Horrocks, Jr., *Inorg. Chem.*, **10**, 1474 (1971).
- (12) As is conventional in this field, the equatorial carbonyl groups are defined as those which are trans to the ER₃ ligands.
- (13) This program, ISOC, was originally written by R. S. Gay and E. H. Brooks of this department and has been in routine use for over 8 years.
- (14) J. D. Cotton, S. A. R. Knox, I. Paul, and F. G. A. Stone, *J. Chem. Soc. A*, 264 (1967).
- (15) O. Kahn and M. Bigorgne, *C. R. Hebd. Seances Acad. Sci., Ser. C*, **262**, 2483 (1965).
- (16) F. Hein and W. Jehn, *Justus Liebigs Ann. Chem.*, **684**, 4 (1965).
- (17) R. Kummer and W. A. G. Graham, *Inorg. Chem.*, **7**, 1208 (1968).
- (18) K. Noack and M. Ruch, *J. Organomet. Chem.*, **17**, 309 (1969).
- (19) R. J. Doedens and J. A. Ibers, *Inorg. Chem.*, **6**, 204 (1967).
- (20) D. T. Cromer and J. B. Mann, *Acta Crystallogr., Sect. A*, **24**, 321 (1968).
- (21) R. F. Stewart, E. R. Davidson, and W. T. Simpson, *J. Chem. Phys.*, **42**, 3175 (1965).
- (22) D. T. Cromer and D. Liberman, *J. Chem. Phys.*, **53**, 1891 (1970).
- (23) R. Hoffmann, J. M. Howell, and A. R. Rossi, *J. Am. Chem. Soc.*, **98**, 2484 (1976).
- (24) Using the crude estimates of σ -donor properties based on force constants,²⁵ one calculates the σ parameter for SiMe₃ groups as -0.84^{26} compared with -0.59 for SnPh₃.²⁵
- (25) W. A. G. Graham, *Inorg. Chem.*, **7**, 315 (1968).
- (26) The force constant calculation is based on band positions of Me₃SiMn(CO)₅ at 2094 (A₁), 2001 (A₁), and 1992 (E) cm⁻¹, as reported by W. Jetz, Ph.D. Thesis, University of Alberta, Edmonton, 1970.
- (27) The van der Waals half-thickness of an aromatic ring is 1.85 Å, whereas the van der Waals radius for a methyl group is 2.0 Å: F. A. Cotton and G. Wilkinson, "Advanced Inorganic Chemistry", 3rd ed, Interscience, New York, N.Y., p 120.
- (28) A compilation is given by P. G. Harrison, T. J. King, and J. A. Richards, *J. Chem. Soc., Dalton Trans.*, 2097 (1975).
- (29) H. P. Weber and R. F. Bryan, *Acta Crystallogr.*, **22**, 822 (1967).
- (30) F. Hein and E. Heuser, *Z. Anorg. Allg. Chem.*, **254**, 139 (1947); **255**, 125 (1947).
- (31) L. E. Orgel, *Inorg. Chem.*, **1**, 25 (1962).
- (32) H. A. Bent, *Chem. Rev.*, **61**, 275 (1961).
- (33) The values of Table IX were estimated from the coalescence temperature and the low-temperature limiting axial-equatorial chemical shift difference.¹ In ref 1 it was noted that in these simple spectra, the values estimated in this way are in excellent agreement with the results of more elaborate simulation methods.
- (34) D. L. Lichtenberger, D. R. Kidd, P. A. Loeffler, and T. L. Brown, *J. Am. Chem. Soc.*, **98**, 629 (1976).
- (35) L. Kruczynski and J. Takats, *Inorg. Chem.*, **15**, 3140 (1976), have correlated chemical shifts with free energies of activation for carbonyl permutation in a series of (1-4- η -diene)tricarbonyliron complexes. The trend is qualitatively the same as in the iron-tin complexes, which may be coincidental in view of the wide difference in the systems.
- (36) R. Ball and M. J. Bennett, *Inorg. Chem.*, **11**, 1086 (1972).

Contribution from the Laboratoire de Chimie de Coordination du CNRS, BP 4142, 31030 Toulouse Cedex, France

Dinuclear-Bridged d⁸ Metal Complexes. 6. Crystal and Molecular Structure and Infrared Study of [Rh(SC₆H₅)(CO)(P(CH₃)₃)₂]₂¹

J.-J. BONNET, P. KALCK, and R. POILBLANC*

Received November 3, 1976

AIC607938

The crystal and molecular structure of *cis*-di(μ -phenylthiolato)-dicarbonylbis(trimethylphosphine)dirhodium (I) has been determined from a single crystal by use of x-ray crystallographic methods. The space group is *P*₂₁/*c* with *a* = 13.843 (6), *b* = 16.912 (8), *c* = 11.235 (5) Å, β = 96.66 (7)°, *Z* = 4. Parameters of 28 nonhydrogen atoms in the asymmetric unit were refined by full-matrix least-squares techniques to a conventional *R* factor of 0.045. In a dinuclear unit, each rhodium atom is in a square-planar environment being bonded to a carbon atom of a carbonyl group, a phosphorus atom of a trimethylphosphine ligand, and two bridging sulfur atoms of two phenylthiolato groups. The dihedral angle of 113° between such two square planes leads to a "bent" geometry with an intramolecular rhodium-rhodium distance of 3.061 (1) Å. The compound is in the anti conformation with respect to the Rh₂(SC₆H₅)₂ core and the phenyl group in the exo position lies between the phosphine ligands. On the basis of the x-ray structure the infrared spectra in the solid state are interpreted by using the factor group approach. In addition an isomerization phenomenon in solution is discussed.

Introduction

From a previous infrared and NMR study¹ the [Rh(SR)(CO)(PA₃)₂]₂ coordination compounds have been shown to have a "bent" double square planar structure. When SR are the *tert*-butylthiolato bridging groups, the compounds were suggested to exist in the *cis* configuration either in solution or in the solid state. Nevertheless for the parent phenylthiolato complexes, various isomers were detected in solution and thus unambiguous conclusions about their geometry were not easy to set up, especially for the compound where PA₃ = P(CH₃)₃; indeed this dicarbonyl complex exhibits three CO stretching bands in the solid state.

For these reasons, it was of interest to undertake an x-ray structural determination of [Rh(SC₆H₅)(CO)(P(CH₃)₃)₂]₂ and thus to compare its geometry with that of [RhCl(C(O)(P(CH₃)₂C₆H₅))₂] previously described.² Moreover, by analysis of the observed differences in the M₂X₂ core an attempt was made to evaluate the factors governing the geometry of dinuclear-bridged d⁸ metal complexes of these and closely related compounds.

Experimental Section

[Rh(SC₆H₅)(CO)(P(CH₃)₃)₂]₂ was prepared as previously described.¹ The crystallization was performed in toluene to which hexane was added without mixing. Suitable crystals were obtained when the mutual diffusion of both solvents is carried out at -20 °C.

Infrared Studies. The infrared spectra were recorded with a Perkin-Elmer 225 grating apparatus equipped with a scale expander in optical density. Cyclohexane solutions or cesium bromide dispersions were used. In the ν_{CO} region of interest, the spectra were calibrated by water vapor lines. Line shape analyses were performed with a Du Pont 310 curve resolver. The part due to diffusion was very small and therefore neglected without any consequence on the Lorentz shape analysis (Chart I).

Data Collection. Diffraction data were collected at room temperature (22 °C) with an Enraf-Nonius CAD 4 computer-controlled four-circle diffractometer. Graphite-monochromatized Mo K α radiation and a take-off angle of 4.5° were used. Intensities were collected using the ω -2 θ scan technique. The scan width was 1° + 0.35 tan θ ; the counter aperture was 3.0 mm in width. Background measurements were obtained during a scan, at each end of the scan interval, with a total duration equal to half of the scan time. A total of 4114 intensities ($\pm h, k > 0, l > 0$) of independant reflections were